

A Universal Technique for Analysis of Acoustic Waves in Periodic Grating Sandwiched Between Multi-Layered Structures and Its Application to Different Types of Waves

Natalya Naumenko
 Moscow Steel and Alloys Institute, Moscow, Russia
nnaumenko@ieee.org

Abstract —A numerical technique, which combines FEM analysis of electrode area with matrix formalism applied to spectral domain analysis (SDA) of eigen modes in multi-layered substrate and multi-layered dielectric upper half-space, is described as an efficient tool of investigating the wave characteristics in periodic metal grating sandwiched between two multi-layered half-spaces, with arbitrary thickness of each layer. The universal character of the developed technique is illustrated by few examples of its application to different types of structure providing propagation of common SAW, boundary waves at interface, plate modes, normal modes in a thin film deposited over the grating etc. The transformation between the waves with continuously increasing film thicknesses can be observed.

I. INTRODUCTION

The rapid growth of modern telecommunication market in the last two decades gave rise to the development of design tools for radiofrequency (RF) resonator-type SAW filters widely used in communication systems. The rigorous simulation of wave characteristics in the periodic grating on top of piezoelectric substrate requires combination of a numerical technique, such as Finite-Element-Method (FEM), to take into account mass load and generally complicated shape of electrodes, and analysis of acoustic fields in piezoelectric substrate. Two well-known methods, FEM-BEM and FEMSDA, are exploited today by many researchers [1-2] and enable accurate simulation of resonator-type SAW devices.

In the last few years, the new impulse in the development of simulation techniques was given by achievements of thin-film technology: thin layers of piezoelectric or dielectric materials with stable and reproducible characteristics can be successfully used today to provide a combination of SAW characteristics, which cannot be achieved in any known substrate material. With variation of material structure and boundary conditions, acoustic waves change their nature and can require modified method of analysis. For example, in the software FEMSDA, which is very popular among researchers, different versions are employed for analysis of dielectric overlay, when it is thin and when its thickness tends to infinite value. It makes difficult to achieve convergence between two versions with continuously growing overlay thickness. It would be helpful to have a universal numerical technique capable to analyze layered structures with arbitrary thickness

of each layer, in order to optimize the film thickness with required wave characteristics, as well as to understand more about physics of wave transformation from one type into another. The present paper describes such technique and gives few examples of its application to multi-layered structures, in which different types of acoustic waves can propagate.

II. METHOD ‘SDA-FEM-SDA’

The approach, which was previously developed for analysis of acoustic modes in multi-layered structures with uniform metal film at the interface [3], has been extended to metal gratings sandwiched between two generally multi-layered half-spaces. The analyzed structure is schematically shown in Fig.1. It is divided into three areas along vertical axis, according to the method of analysis applied to each area. FEM is employed in the electrode region, which is confined between $z=0$ and $z=h$. In the upper ($z>h$) and lower ($z<0$) multi-layered half-spaces, analysis is performed in spectral domain. Such method can be called “SDA-FEM-SDA”, to emphasize the main feature, which distinguishes it from FEMSDA: the dielectric overlay is not included in FEM. Similar to the substrate, this area is analyzed in spectral domain.

Other important features, which provide a universal character of the developed numerical technique and the software based on this technique, are described below.

1) The characteristics of partial waves propagating in each material layer are found as eigen vectors and eigen values of a fundamental acoustic tensor, which depends on material constants of the layer and its orientation. Such numerical

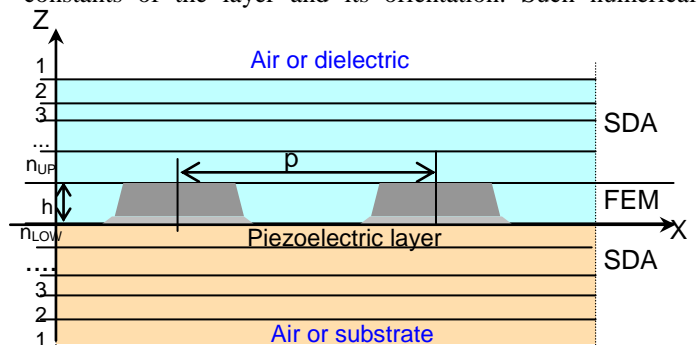


Fig.1. Schematic drawing of analyzed structure

technique is **insensitive to degeneracy of SAW** (e.g. due to symmetry), in the analyzed orientation.

2) Analysis starts from the uppermost or lowermost half-infinite layer, where the wave structure is calculated. In each adjacent finite-thickness layer, the transformation of the wave structure is deduced via separate treatment of incident and reflected partial modes. Hence, the reflection and transmission matrix coefficients [2] replace the transfer matrix, which is known to be bad conditioned for layer thickness exceeding 3-5 wavelengths. As a result, robust analysis of multiple layers with **arbitrary thicknesses** is provided.

3) To simulate the propagation of acoustic waves in a grating deposited on top of thin (few wavelengths) piezoelectric plate or at the interface between the substrate and thin dielectric overlay, stress-free mechanical boundary conditions can be simulated at certain interface by specifying very low values of elastic constants and mass density of the adjacent material (air). Hence, the same numerical procedure enables analysis of **plate modes**. In addition, continuous transformation of certain mode in the grating from SAW into **boundary wave** can be observed with increasing dielectric film thickness. It should be mentioned that the general numerical procedure of finding eigen modes of fundamental acoustic tensor can be successfully applied to such rare and isotropic medium as air and the results of analysis do not differ noticeably from that obtained with stress-free conditions set analytically.

SDA analysis of lower and upper half-spaces is considered completed when the wave structure has been finally determined at $z=0$ and $z=h$ and the impedance matrices $\hat{Z}_{UP}(k_n)$ and $\hat{Z}_{LOW}(k_n)$ have been calculated. These matrices characterize the ratio between the vectors of displacement $\mathbf{u}(k_n)$ and normal stress $\mathbf{T}(k_n)$ of partial waves propagating along the interface and having tangential component of the wave vector $k_n = k_0 + 2\pi n$ ($n=-N, \dots, +N$), where n is the number of Floquet harmonic. In piezoelectric (top surface of the lower half-space), each vector is 4-dimensional, with added electrostatic potential φ and normal electrical displacement D ,

$$\begin{pmatrix} \mathbf{u} \\ \varphi \end{pmatrix} = \hat{Z}_{LOW} \begin{pmatrix} \mathbf{T} \\ D \end{pmatrix} = \begin{pmatrix} Z_{LOW}^{11} & Z_{LOW}^{12} \\ Z_{LOW}^{21} & Z_{LOW}^{22} \end{pmatrix} \begin{pmatrix} \mathbf{T} \\ D \end{pmatrix},$$

The matrices $\hat{Z}_{UP}(k_n)$ and $\hat{Z}_{LOW}(k_n)$ are further inserted in two boundary conditions,

$$\begin{aligned} \hat{T}_0^{FEM}(x_i^0) &= \hat{G}_0^{-1}(x_k, k_n) \cdot (\hat{Z}_{LOW}^{11})^{-1} \cdot \hat{G}_0(k_n, x_i) \cdot \hat{u}_0^{FEM}(x_i^0) + \\ &+ \hat{G}_0^{-1}(x_k, k_n) \cdot (\hat{Z}_{LOW}^{11})^{-1} \cdot \hat{Z}_{LOW}^{12} \cdot Q(k_n), \quad z=0 \end{aligned}$$

and

$$\hat{T}_h^{FEM}(x_i) = \hat{G}_H^{-1}(x_k, k_n) \cdot (\hat{Z}_{UP})^{-1} \cdot \hat{G}_H(k_n, x_i) \cdot \hat{u}_h^{FEM}(x_j), \quad z=h$$

where $\hat{G}_0(k_n, x_i)$ and $\hat{G}_H(k_n, x_i)$ denote conversion from the x -dependent variables assigned to the nodal points into $\mathbf{u}(k_n)$ and $\mathbf{T}(k_n)$ in spectral domain, by numerical integration over period of the grating, at $z=0$ and $z=h$, respectively. The nodal

points are generally different at two boundaries, if electrodes are non-rectangular.

The ratio between $\hat{T}_0^{FEM}(x_i)$, $\hat{u}_0^{FEM}(x_j)$, $\hat{T}_h^{FEM}(x_i)$ and $\hat{u}_h^{FEM}(x_j)$ is determined from FEM analysis of electrode region, and Blotekjeer's approximation is applied to find the ratio between charges and voltages at $z=0$, as described in [1].

The software SDA-FEM-SDA based on the described numerical technique enables analysis of electrodes composed of few different metal layers and having a complicated profile, with different edge angle in each metal layer. Fig.1 shows an example of two-layered electrodes. The gaps between electrodes may be empty or filled with dielectric material. Due to these options, some "thin" effects can be simulated. For example, the effect of sublayer (e.g. titanium) often used for better adherence of electrode metal to the substrate or the effect of nonrectangular electrode profile typical for certain fabrication process can be investigated. Analysis of obliquely propagating waves in the grating helps to estimate the effect of transverse modes (diffraction) on the frequency response of a resonator. The next section gives few examples of application of the developed numerical technique to different multi-layered structures.

III. NUMERICAL EXAMPLES

All numerical examples refer to the same piezoelectric material, langasite (LGS) cut with Euler angles (0° , 22° , 90°), which is combined with dielectric layers, as a substrate, or with non-piezoelectric wafer, as a plate. LGS is known as the best piezoelectric material for high-temperature applications, due to high melting temperature and the absence of phase transitions. Bleustein-Gulyaev wave (BGW) propagating in the analyzed orientation is expected to show small temperature coefficient of frequency (TCF) combined with sufficiently high piezoelectric coupling, when the substrate is utilized in SAW resonator. Therefore, in addition to demonstrate abilities of the new simulation tools, numerical examples given in the next section can contribute the topical research of langasite as material for RF SAW sensors operating in wide range of temperatures, up to 700°C .

A: LGS substrate with Pt grating.

Due to high melting point, platinum (Pt) is the best candidate for high temperature applications. Thin zirconium (Zr) sublayer ($0.1\% \lambda$ in the analyzed example, where $\lambda=2p$) helps to improve adhesion, instead of titanium (Ti) commonly used for the same purpose at lower temperatures [4]. All calculations were made with material constants of LGS reported in [5] and average values of reported Pt and Zr constants. In Fig.2, the "effective" velocity is presented, which was estimated at resonant frequency f_R , as $V_R=2pf_R$. With Pt thickness growing from zero up to $5\% \lambda$, the velocity goes down. TCF shows small negative values reaching $-6 \text{ ppm}/^\circ\text{C}$ for $h_{Pt}=5\% \lambda$. Simulations for Pt rectangular electrodes are compared with Pt/Zr electrodes having edge angles 75° and 45° , respectively. The difference grows with Pt thickness.

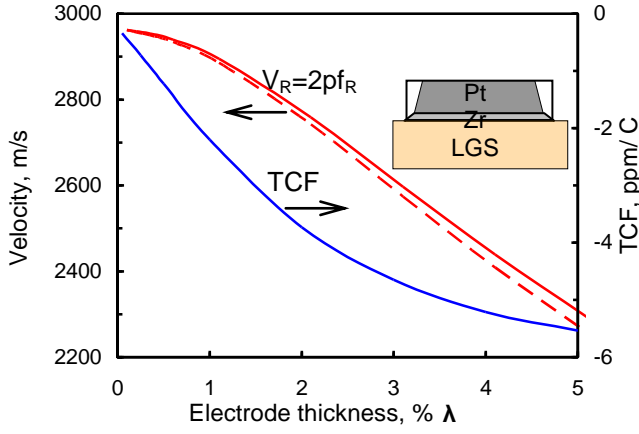


Fig.2. Effective velocity and TCF of SH-type SAW, estimated at resonant frequency, in LGS, (0° , 22° , 90°), as functions of electrode thickness. Solid lines refer to Pt/Zr electrodes with fixed Zr thickness $0.1\% \lambda$ and shown profile, dashed lines refer to Pt electrodes (rectangular area), with $a/p=0.5$.

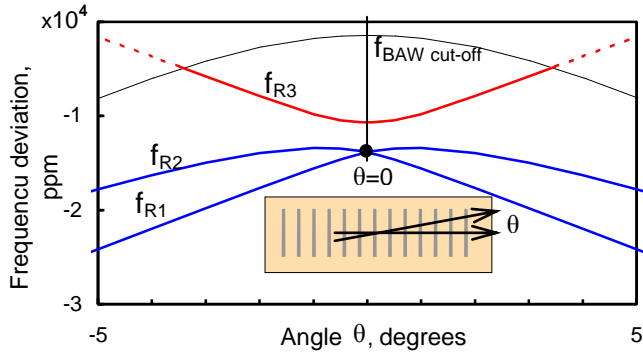


Fig.3. Variation of resonant frequencies $\Delta f/f_0$ for obliquely propagating waves, in LGS, (0° , 22° , 90°) with Pt grating, $h_{Pt}=1\% \lambda$.

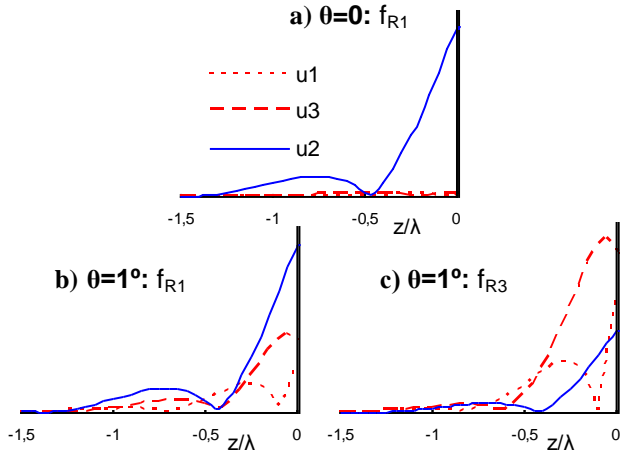


Fig.4. Transformation of the wave structure (displacement fields in the depth of LGS) for two branches, which arise from SH-type mode with increasing oblique propagation angle, in LGS, (0° , 22° , 90°) with Pt electrodes, $h_{Pt}=1\% \lambda$.

Example of variation of resonant frequency with the angle of oblique propagation θ is shown for the same LGS orientation in Fig.3. With increasing θ , the admittance $Y(f)$

shows three resonances instead of one. Analysis of the wave structure (Fig. 4) at $\theta=0$ and $\theta=1^\circ$ reveals that they result from interaction between two SAW modes in the grating, one of which modifies into leaky SAW at $\theta=3.5^\circ$. The coupling of two SAW modes with small deviation of propagation direction from X-axis of the substrate can affect the resonator characteristics and should be taken into account.

B: LGS substrate with Pt grating and SiO_2 overlay

Dielectric silicon dioxide (SiO_2) film is often used for passivation, to protect electrode structure from environmental influence. Due to positive TCF, thin SiO_2 film helps to improve temperature characteristics in most of piezoelectric materials. In (0° , 22° , 90°)-LGS with Pt electrodes, $h_{Pt}=2\% \lambda$, the calculated $\text{TCF}=-3.7 \text{ ppm}/^\circ\text{C}$. When SiO_2 is deposited between electrodes with flattened top surface, TCF shifts to $-0.4 \text{ ppm}/^\circ\text{C}$ (Fig.5a). With further increasing film thickness (measured from top of electrode), TCF crosses zero value at $h_{\text{SiO}_2}=0.3\% \lambda$. The velocity V_R slowly grows with increasing h_{SiO_2} . Considering this example is not aimed at accurate prediction of SiO_2 thickness for temperature compensated characteristics, because such prediction would require very accurate values of all material constants. However, it reveals another application of the developed technique.

C: LGS substrate with Pt grating and $\text{SiO}_2/\text{Al}_2\text{O}_3$ overlay

The next example demonstrates application of the method and software to two-layered upper dielectric deposited over LGS with Pt grating. The second layer is aluminum dioxide Al_2O_3 , a material with very high thermal conductivity. It can help reduce the effect of high temperatures on LGS surface and metal structure. Thin SiO_2 film between LGS and Al_2O_3 can help promote adherence between dissimilar materials, such as LGS and Al_2O_3 . In Al_2O_3 acoustic waves propagate with high velocities and with increasing its thickness the velocity of SAW mode grows fast until it merges with SH-BAW in LGS, at $h=2.2\% \lambda$ (Fig.5b). With further increasing $h_{\text{Al}_2\text{O}_3}$, SAW leaks into LGS.

An example of admittance function is presented in Fig.6. Thick Al_2O_3 overlay, $h_{\text{Al}_2\text{O}_3}=4\lambda$, covers thin SiO_2 film, $h_{\text{SiO}_2}=0.2\% \lambda$. Only one mode can be seen in wide interval of velocities, up to 7500 m/s . It is quasi-bulk, with velocity close to $V_{\text{SH-BAW}}$ in LGS, and leaks into LGS.

D: LGS plate bonded to silicon wafer

The last numerical example refers to thin piezoelectric plate (LGS) bonded to non-piezoelectric silicon (Si) wafer. Pt grating generates waves in LGS, and the number of plate modes increases with LGS thickness (Fig.7). These modes look as regular ripples in admittance of the grating (Fig.8). To avoid electric currents in silicon wafer, intermediate film can be introduced between LGS plate and Si and simulated with the tools described in the paper.

Two more examples can be found in [6], with Cu grating sandwiched between SiO_2 and 128°YX or YX-LN . The transformation of SAW into boundary waves is observed via

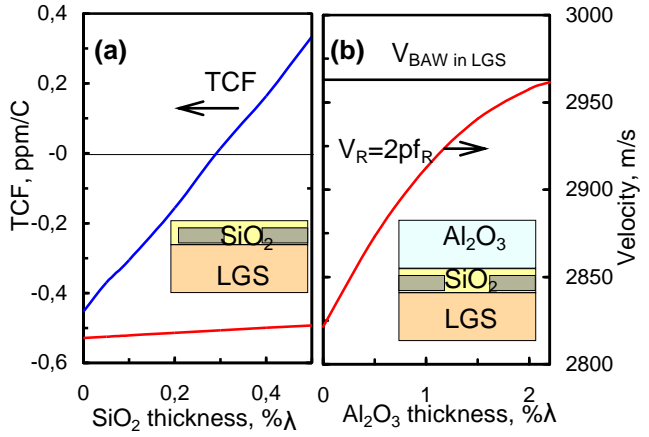


Fig.5. Velocity and TCF at resonant frequency, in SiO₂/Pt grating/LGS as functions of SiO₂ thickness (a) and velocity in Al₂O₃/SiO₂/Pt grating/LGS, with fixed $h_{SiO_2}=0.5\%λ$, as function of Al₂O₃ thickness (b), $h_{Pt}=2\%λ$.

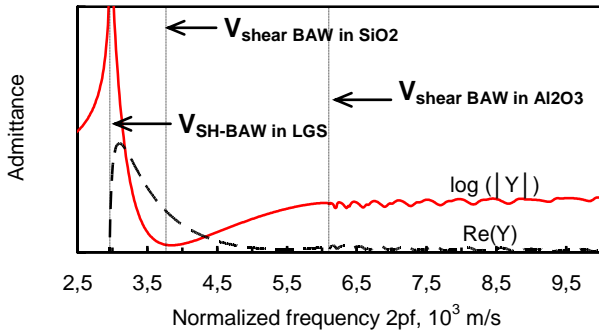


Fig.6. Calculated admittance of platinum grating, $h_{Pt}=2\%λ$, at the interface between LGS and two-layered SiO₂/Al₂O₃ upper dielectric, with $h_{SiO_2}=0.2\%λ$ and $h_{Al_2O_3}=4λ$.

numerical simulation of acoustic fields in the layered structure.

IV. CONCLUSION

The developed numerical technique SDA-FEM-SDA is a universal tool, which provides investigation of different types of acoustic waves propagating in periodic grating sandwiched between two generally multi-layered structures.

The software SDA-FEM-SDA was developed for TriQuint Semiconductors, Inc. and its efficiency, robustness and accuracy of simulation was verified experimentally.

ACKNOWLEDGEMENT

The author thanks Ben Abbott for many useful discussions and experimental verification of the developed tools. Also, the author thanks all participants of SAWHOT coordinated project on wireless SAW sensors for the idea of applying numerical technique to langasite as material for such sensors.

REFERENCES

[1] G. Endoh, K. Hashimoto, and M. Yamagouchi, "SAW Propagation Characteristics by Finite Element Method and Spectral Domain Analysis", *Jpn.J.Appl.Phys.*, vol.34, No 5B, pp.2638-2641, 1995.

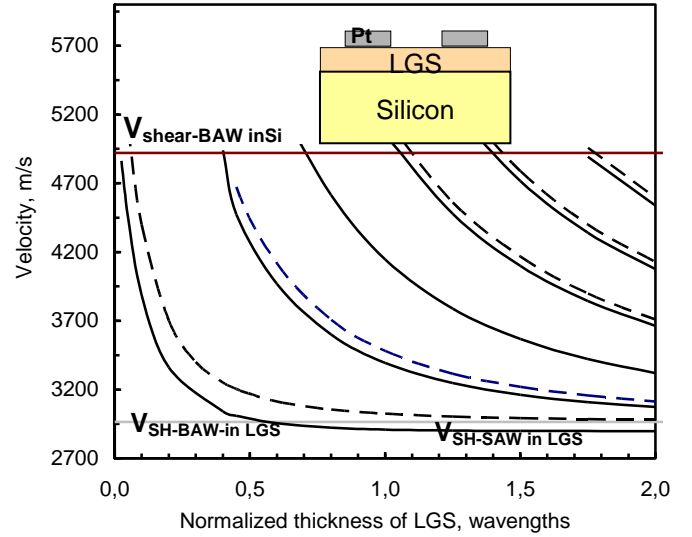


Fig.7. Effective velocities of acoustic modes propagating in Pt grating ($h=1\%λ$) on LGS plate, ($0^\circ, 22^\circ, 90^\circ$), bonded to silicon wafer, as function of LGS plate thickness

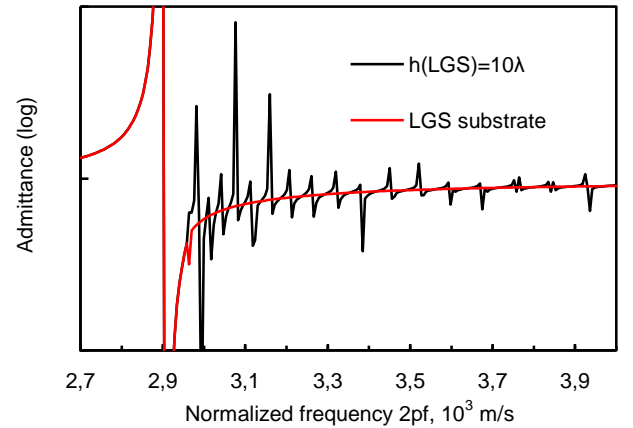


Fig.8. Calculated admittance of platinum grating, $h_{Pt}=1\%λ$, on LGS plate, $h=10λ$, bonded to Si wafer (black line), compared to the case of LGS substrate (red line).

[2] S. Ballandras, A. Reinhardt, L. Laude, A. Soufyane, S. Camou and P. Ventura, "Simulations of surface acoustic wave devices built on stratified media using mixed finite element/boundary integral formulation", *J.Appl.Phys.*, v.96, No 12, pp.7731-7741, 2004.

[3] N. Naumenko, "Transformation of Surface Acoustic Waves into Boundary Waves in Piezoelectric/Metal/ Dielectric Structures", in *Proc. IEEE Ultrason. Symp.*, 2009, pp. 2635-2638.

[4] J.A. Thiele, and M. Pereira da Cunha, "Platinum and Palladium High-Temperature Transducers on Langasite", *IEEE Trans. Ultrason. Ferroelectr. Freq. Contr.*, vol. 52, no. 4, pp. 545-549, 2005.

[5] A. Bungo, C. Jian, K. Yamaguchi, Y. Sawada, R. Kimura, and S. Uda, "Experimental and theoretical analysis of SAW properties of the Langasite Substrate with Euler Angle ($0^\circ, 140^\circ$, f)", in *Proc. IEEE Ultrasonics Symp.*, pp 231-234, 1999.

[6] N. Naumenko, and B. Abbott "Insight into the Wave Transformation Mechanisms via Numerical Simulation of Acoustic Fields in Piezoelectric/Metal Grating/Dielectric Structures", to be published in *Proc. IEEE Ultrason. Symp.* 2010.